LAWRENCE
LIVERMORE
NATIONAL
LABORATORY

LLNL-TR-407872

Initial Aging Studies of Unfilled VCE

S. E. Letant, J. L. Herberg, T. S. Wilson, C. T. Alviso, S. C. Chinn, R. S. Maxwell

October 16, 2008

Disclaimer

This document was prepared as an account of work sponsored by an agency of the United States government. Neither the United States government nor Lawrence Livermore National Security, LLC, nor any of their employees makes any warranty, expressed or implied, or assumes any legal liability or responsibility for the accuracy, completeness, or usefulness of any information, apparatus, product, or process disclosed, or represents that its use would not infringe privately owned rights. Reference herein to any specific commercial product, process, or service by trade name, trademark, manufacturer, or otherwise does not necessarily constitute or imply its endorsement, recommendation, or favoring by the United States government or Lawrence Livermore National Security, LLC. The views and opinions of authors expressed herein do not necessarily state or reflect those of the United States government or Lawrence Livermore National Security, LLC, and shall not be used for advertising or product endorsement purposes.

This work performed under the auspices of the U.S. Department of Energy by Lawrence Livermore National Laboratory under Contract DE-AC52-07NA27344.

INITIAL AGING STUDIES OF UNFILLED VCE

Sonia E. Létant, Julie L. Herberg, Thomas S. Wilson, Cynthia T. Alviso, Sarah C. Chinn, and Robert S. Maxwell

Abstract

This report presents initial data on the effects of temperature, oxygen, and radiation on the chemical and structural properties of newly formulated, unfilled VCE. This initial effort focused on a pristine sample, and a replicate sample irradiated in air at a dose of 25MR.

Thermal degradation was investigated by performing Thermogravimetric Analysis (TGA), and radiation-induced degradation was investigated using Differential Scanning Calorimetry (DSC), X-ray Diffraction (XRD), Solid Phase MicroExtraction – Gas Chromatography/Mass Spectrometry (SPME-GC/MS), as well as various Nuclear Magnetic Resonance (NMR) techniques including: ^{13}C, ^{13}C {^{1}H} cross polarization (CP), and ^{1}H magic angle spinning (MAS) NMR.

Table of content

1. Introduction 2
2. Experimental Approach 2
3. Results and Discussion 2
   3.1. Thermal degradation of VCE 3
      3.1.1. Thermogravimetric Analysis (TGA) 3
   3.2. Radiation-induced degradation of VCE 4
      3.2.1. Structural effects 4
      3.2.1.1. Differential Scanning Calorimetry (DSC) 4
      3.2.1.2. X-Ray Diffraction (XRD) 6
      3.2.2. Chemical effects 6
      3.2.2.1. Solid Phase Microextraction – Gas Chromatography/Mass Spectrometry (SPME-GC/MS) 6
      3.2.2.1. Nuclear Magnetic Resonance (NMR) 9
4. Conclusion 12
5. Future work 13
5. References 14

1. Introduction

VCE is an ethylene/vinyl acetate/vinyl alcohol terpolymer binder for filled elastomers (Figure 1) which is designed to accept high filler loadings in rubber compounds. Material characterization and aging studies had been performed on previous formulations of this material [1-2] but the Ethylene Vinyl Acetate (EVA) starting copolymer is no longer commercially available. New formulations with replacement EVA materials are currently being established and will require characterization as well as updated aging models [3, 4].

This report presents initial data on the effects of temperature, oxygen, and radiation on the chemical and structural properties of newly formulated, unfilled VCE.

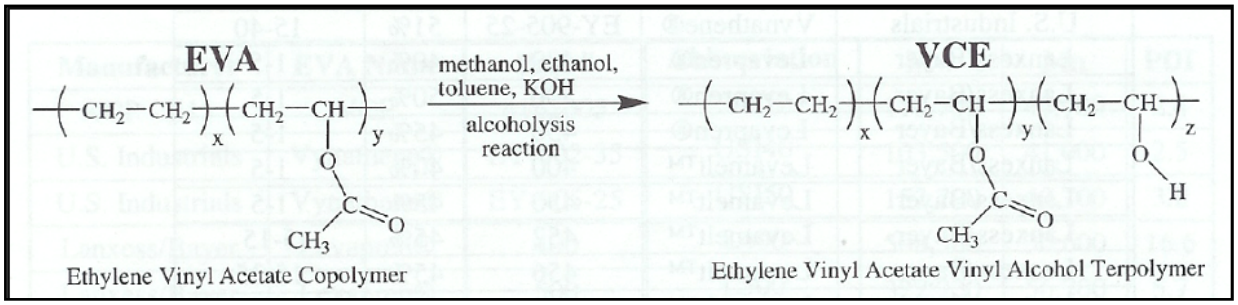

Figure 1: Base catalyzed alcoholysis reaction of EVA copolymer yielding VCE [3]. Typical VCE composition is 34.9-37.9% vinyl acetate, and 1.27-1.78% hydroxyl.

2. Experimental Approach

Initial aging studies were performed on a VCE formulation prepared at LANL. One VCE sample was set aside (pristine), while the other was sealed with air into a plastic bag, placed into a stainless steel vessel, and exposed to a 1.2 MeV, 5kGray/hour, ^{60}C source and irradiated to 250 kGray (25MR). While samples irradiated with intermediate doses (1, 5, 10 MR) were also prepared, this initial effort focused on the two extremes: a pristine sample, and a sample irradiated in air at a dose of 25MR.

Thermal degradation was investigated by performing Thermogravimetric Analysis (TGA), and radiation-induced degradation was investigated using Differential Scanning Calorimetry (DSC), X-ray Diffraction (XRD), Solid Phase MicroExtraction – Gas Chromatography/Mass Spectrometry (SPME-GC/MS), as well as various Nuclear Magnetic Resonance (NMR) techniques including: ^{13}C, ^{13}C $\{^{1}H\}$ cross polarization (CP), and ^{1}H magic angle spinning (MAS) NMR.

3. Results and Discussion

Potential sources of chemical or structural degradation and their effects need to be identified prior to using VCE as a binder in engineering applications, particularly in enduring systems. Typical sources of degradation addressed in this report are isolated or combined exposures to oxygen, high temperatures, and gamma radiation. Such exposures have been reported to cause chemical modifications (production of volatile degradation products, incorporation of oxygen) as

well as structural modifications (main chain scission, cross-linking, end-linking) in polymer materials.
Recent publications showed that ethylene vinyl alcohol (EVOH) copolymers, which are similar to VCE, were affected by electron and gamma radiation. EVOH was shown to scavenge oxygen in the presence of electron or gamma irradiation (electrons create radicals, which allows oxygen to react with the polymer to form aldehydes and ketones) [5]. In addition, the material was shown to be less crystalline [5], and more cross-linked [6] after irradiation.
Reported effects of electron and gamma radiation on EVA copolymers also include oxygen incorporation and increased cross-linking [7,8].
To the best of our knowledge, there is no published data to date on the degradation of VCE terpolymers.

3.1. Thermal degradation of VCE

3.1.1. Thermogravimetric Analysis (TGA)

TGA experiments were performed on a Perkin Elmer TGA-7, under a flow of nitrogen gas of 20 mL/min. Approximately 3 mg of each sample were heated from 50 ºC to 900 ºC with a ramp rate of 10 ºC /min and the change in weight percent was plotted as a function of temperature.

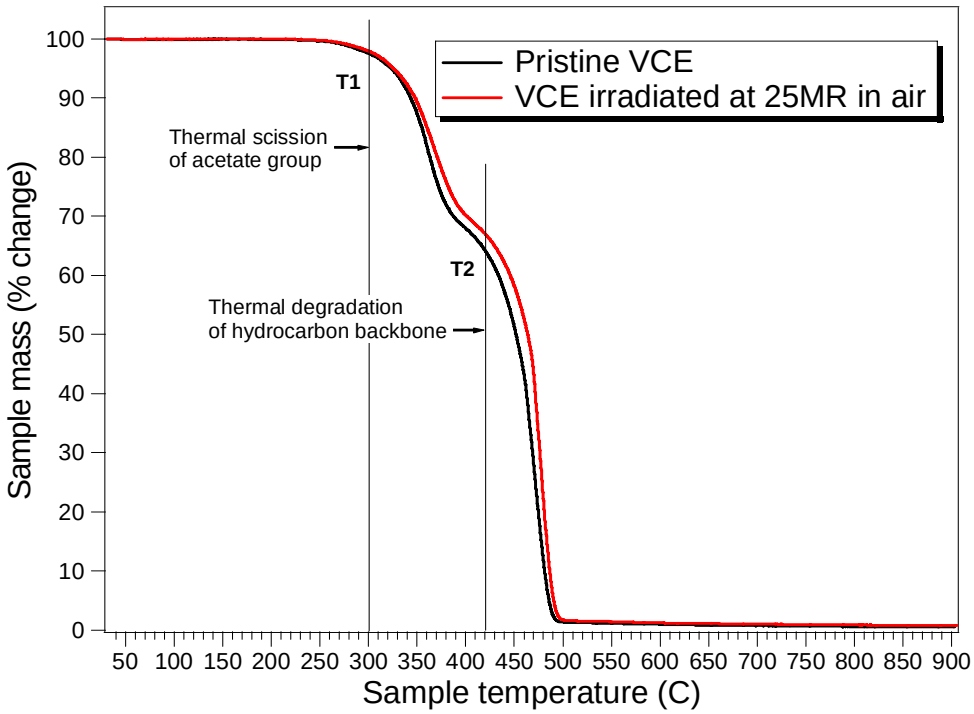

Figure 2: TGA curves for pristine and irradiated VCE samples. The change in weight percent is plotted as a function of the temperature for each sample.

TGA experiments performed on both pristine and 25MR irradiated VCE samples (Figure 2) showed that no significant thermal degradation occurs below 300 ºC. Thermal scission of the acetate group was observed at 315 ºC, followed by the thermal degradation of the hydrocarbon

backbone at 420 ºC (main chain degradation). There were no significant differences between the thermal degradation curves of pristine and irradiated VCE.

3.2. Radiation-induced degradation of VCE

3.2.1. Structural effects

3.2.1.1. Differential Scanning Calorimetry (DSC)

DSC experiments were performed using a Perkin Elmer Diamond instrument, under a flow of nitrogen gas of 20 mL/min. Samples were placed into aluminum pans, weighed, and submitted to the following temperature cycle: 2 min at 25 ºC, 25 to 200 ºC at 20 ºC/min, 2 min at 200 ºC, 200 to -60 ºC at 20 ºC/min, 5 min at -60 ºC, and -60 to 200 ºC, 20 ºC/min. Thermograms were base line-corrected to remove the contribution from the aluminum pans.

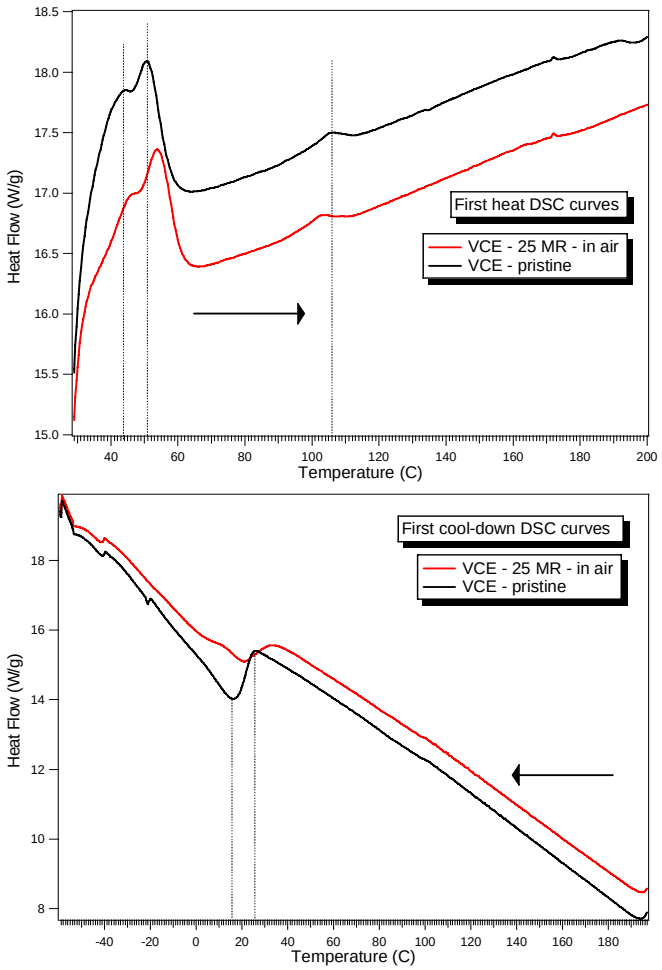

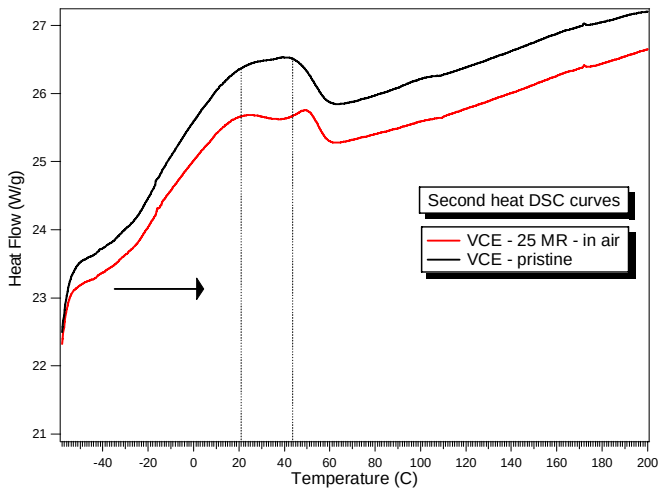

Figure 3: DSC curves for pristine and irradiated VCE samples. Top: first heat, middle: first cool down, bottom: second heat.

Although thermogram peaks are complex for the VCE terpolymer, due to overlapping transitions of the copolymer/monomer components, DSC experiments (Figure 3) revealed qualitative differences between pristine and irradiated VCE samples including: a shift of the melting transition temperature (T_m), which indicates a change in mobility, a decrease in enthalpy of fusion (ΔH_f), which indicates a decrease in crystallinity after irradiation, and finally, broadened transitions (larger peak areas), which indicates less uniformity and a higher level of cross-linking after irradiation. Table 1 provides a quantitative summary of the differences between pristine and irradiated VCE materials, as well as crytallinity percentages calculated from the experimental values of the enthalpies of fusion (8.3% for pristine VCE, and 5.6 % for gamma-irradiated VCE). Such low crystallinity percentages should be expected in VCE terpolymers since the acetate content in these materials is significant. The bulky acetate groups are excluded from the polyethylene crystal lattice, which decreases the fraction of crystallizable units as the vinyl acetate content increases [9].

These results suggest that gamma irradiation of VCE in air may lead to reduced crystallinity, reduced uniformity, and increased cross-linking.

Table 1. Quantitative summary of DSC experiments, comparing properties of pristine and irradiated VCE.

Sample	**T_m (ºC)**	**Peak area (mJ)**	**ΔH_f (J/g)**	**Crystallinity[1] (%)**
Pristine VCE	26.3	148.5	23.6	8.3
Irradiated VCE (25 MR in air)	20.6	92.0	16.1	5.6

[1] % crystallinity = (ΔHf / ΔHf^*) x 100

ΔHf^* = 285.8 J/g for PolyEthylene (Heat of fusion for 100% crystalline sample)[10]

3.2.1.2. X-Ray Diffraction (XRD)

XRD can usually detect crystallinity levels above 5% in polymeric materials. In order to confirm the decrease in crystallinity observed by DSC on irradiated VCE samples, XRD experiments were conducted on both pristine and irradiated samples using a Philips vertical goniometer with Copper Ka radiation. Step scans from 20 to 80° (2θ) with step sizes of 0.02° were used, with a total acquisition time of 4 s.

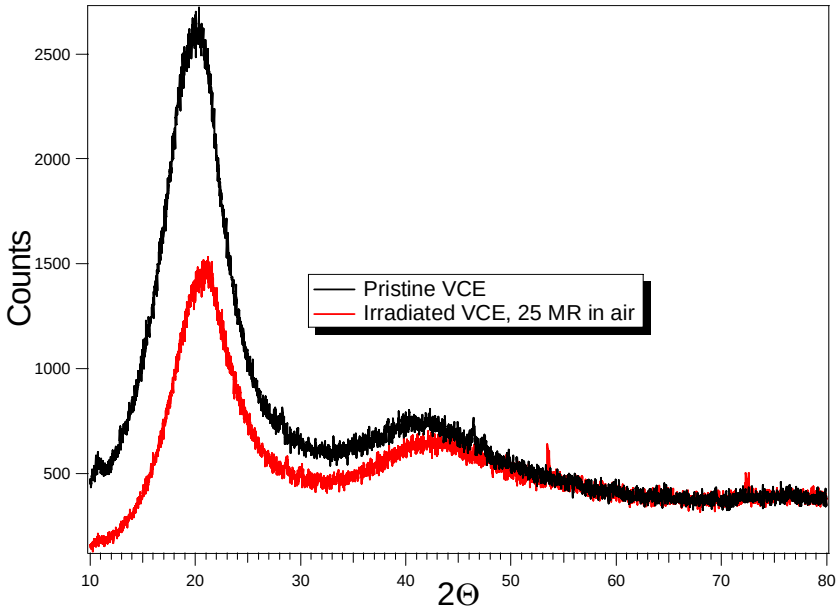

Figure 4: XRD spectra of pristine and irradiated VCE samples acquired at room temperature.

As may be been on Figure 4, XRD did not appear to be sensitive enough to effectively detect the low crystallinity level of the samples. It should also be noted that the diffraction experiments were conducted at room temperature, which is located right on the broad fusion/crystallization peak (see Figure 3; DSC, middle graph). Nevertheless, XRD spectra qualitatively support the DSC data, since the diffraction peak of the pristine VCE sample is more intense and has a smaller FWHM than the diffraction peak of the irradiated VCE, which suggests a higher level of crystallinity for the pristine material.

3.2.2. Chemical effects

3.2.2.1. Solid Phase Microextraction – Gas Chromatography/Mass Spectrometry (SPME-GC/MS)

The samples (20-30 mg each) were placed in SPME headspace vials (20mL), and sealed with crimp caps and septa (20 mm, Teflon/blue silicone, level 4) that were purchased from MicroLiter Analytical Supplies. For each sample type (pristine and 25MR irradiated), one sample was left at room temperature and a duplicate sample was placed in an oven at 70 ˚C. All samples remained

at their designated temperatures for two weeks. An additional set of blanks (sealed empty vials) was also prepared for storage at room temperature and 70 ˚C prior to SPME sampling. The storage at elevated temperatures was performed to maximize the volatilization of degradation signatures for observation by SPME sampling, while retaining a room temperature sample and a blank to serve as controls.

The samples were analyzed by SPME GC/MS using an automated system under the following conditions: 85 µm Carboxen/PDMS SPME fiber (purchased from Supelco), conditioned between samples for 5 min at 260 ˚C; headspace sampled at 50 ˚C for 20 min and injected into the GC for 1 min at 250 ˚C. The Agilent 6890 GC was set for splitless injection and purged at 0.5 min using a J & W Scientific DB-624 column (30 m, 0.25 mm ID, 1.4 µm film) with a constant 1.0 mL/min flow of helium. The 20 min run had the following temperature profile: 40 ˚C/1.05 min, 23.41˚C/min to 260 ˚C, and held 6.81 min. An Agilent 5973 mass spectrometer scanned the mass range from 35-450 at a rate of 1.81 scans/s with no filament delay. Outgassing products were identified by comparison of their mass spectra to the NIST 02 mass spectral library.

Figure 6 shows GC-MS spectra for the 4 samples analyzed. The nature and abundance of the chemicals found in the headspace is summarized in Table 2. The 3 main outgassing chemicals are: acetic acid, phenol, and cyclic siloxanes. Acetic acid is the product of the hydrolysis of the vinyl acetate groups of VCE (see VCE structure shown in Figure 1) into vinyl alcohol groups. Phenol is a degradation product of the crosslinking agent Hylene W (see structure in Figure 5) used in the synthesis of VCE, resulting from thermal unblocking or from hydrolysis of urethane. Cyclic siloxanes could either come from mobile species resulting from the contact with foams, or from release from the silicone mold used during the processing of the samples.

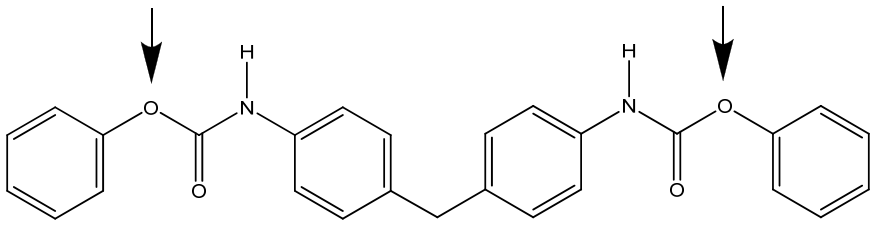

Figure 5: Chemical structure of Hylene MP curing agent (diphenol-4,4', -methylenebis(phenylcarbamate). Arrows indicate the 2 sites where a hydrolysis reaction may lead to the formation of phenol molecules.

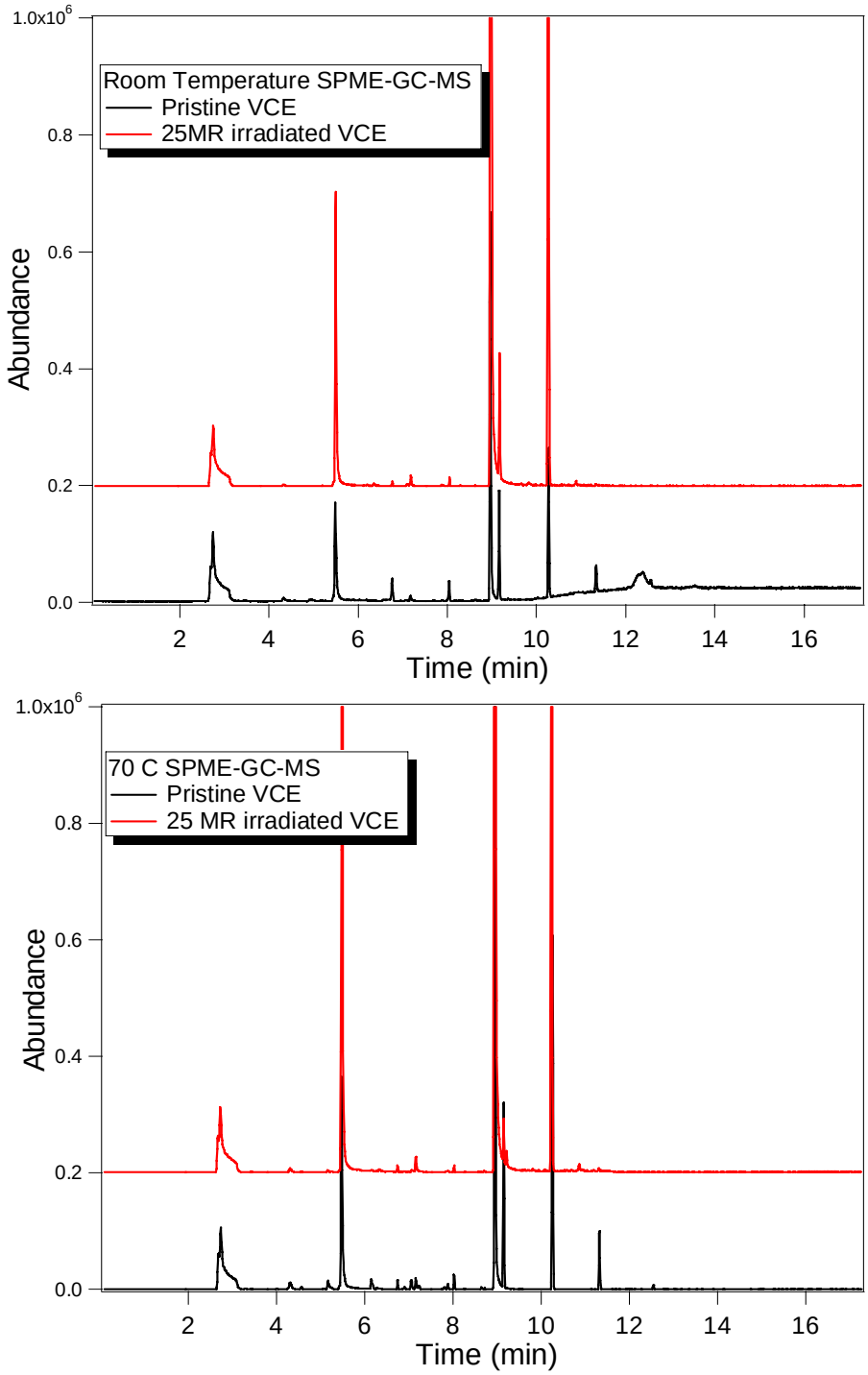

Figure 6: SPME-GC-MS spectra for pristine and irradiated VCE samples at room temperature (top) and at 70˚C (bottom).

Table 2. Quantitative summary of SPME-GC-MS experiments, comparing abundance of outgassing products from both pristine and irradiated VCE at room temperature and at 70 ˚C.

Sample	**Pristine VCE**	**25 MR VCE**	**Pristine VCE**	**25 MR VCE**
Temperature	RT	RT	70 C	70C
Carbon dioxide	5.5 %	1%		1%
Acetic acid	9 %	4.5 %	13%	10.0%
Phenol	26 %	69%	32%	61%
Benzene*		13.5 %		14%
Cyclic siloxanes	14 %	2 %	25%	1%

* Benzene, 1,3-bis(1,1-dimethylethyl)

The quantity of acetic acid released into the headspace does not appear to depend on whether the sample is irradiated or not, which is consistent with the production of acetic acid in the sample via hydrolysis. The outgassing of phenol and 1,3-bis(1,1-dimethylethyl) benzene increases upon irradiation, which may arise from irradiation-assisted cleavage of Hylene MP molecules. Finally, the outgassing of cyclic siloxanes decreases upon irradiation, which may be due to radiation-induced cross-linking in the polymer structure.

3.2.2.1. Nuclear Magnetic Resonance (NMR)

Both the pristine and 25MR irradiated VCE samples were analyzed using 13C, 13C {1H} CP, and 1H MAS NMR, which were performed on a Bruker Avance 400MHz spectrometer with a magnetic field of 9.4T. This provides a resonance frequency of 100.614 MHz for 13C (spin=1/2) and 400MHz for 1H (spin=1/2). The solid samples were placed at the center of a 4mm Bruker rotor. Spinning rates of 12kHz were used. The 13C CPMAS spectra were recorded with a cross polarization experiment [11]. The 13C {1H} CPMAS NMR data were recorded with a 90 degree pulse width of 5s. In these experiments, the relaxation delay was 3s and the number of acquisitions was 4096. The contact time was set to 1ms. The 13C MAS NMR data were recorded with a 90 degree pulse width of 5s. In these experiments, the relaxation delay was 10s and the number of acquisitions was 2048. The 1H MAS NMR data were acquired with a 90 degree pulse width of 5.35s. In these experiments, the relaxation delay was 3s and the number of acquisitions was 32. The 3C {1H} CP and 13C MAS NMR data were referenced to glycine at 32ppm and 176.5ppm. The 1H MAS NMR data were reference to TMS at 0ppm.

Figure 7 shows 13C {1H} CP MAS NMR spectra of pristine and 25MR irradiated VCE samples. The 13C {1H} CP MAS spectra of both samples show a peak at 20.3ppm, which represents aliphatic carbon in the form of CH_3. In addition, the spectra show peaks at 25ppm, 30ppm, 32ppm, and 34ppm, which represent aliphatic carbon in the form of CH_2. The 13C {1H} CP MAS NMR spectra for the pristine and 25MR irradiated VCE do not show significant changes in chemical shift or peak shape, indicating that the aliphatic carbons are very stable and are not significantly impacted by exposure to radiation. In addition, the spectra show peaks at 71ppm and 74ppm, which represent aliphatic carbon in the form of CH. These aliphatic carbon atoms are bound to oxygen, as shown in Figure 7. There does not seem to be a significant change in chemical shift between these two peaks in the 13C {1H} CP MAS NMR spectra for either the

pristine or irradiated VCE samples. However, there is a very slight change in the shape of the peak at 74ppm.

To understand how the carboxyl carbon and the aliphatic carbon are being affected by irradiation, a 13C MAS NMR experiment was performed on both the pristine and 25MR irradiated VCE sample. These spectra are presented in Figure 8 and show one additional peak from the 13C{1H} CP MAS NMR data at 169ppm, which represents a carboxyl carbon (Note that there is a background peak due to the NMR probe at approximately 128ppm). This peak shows no change in chemical shift or peak shape between the 13C MAS NMR spectra of the pristine and 25MR irradiated VCE, which indicates that the carboxyl carbon atoms are very stable and are not significantly impacted by exposure to radiation.

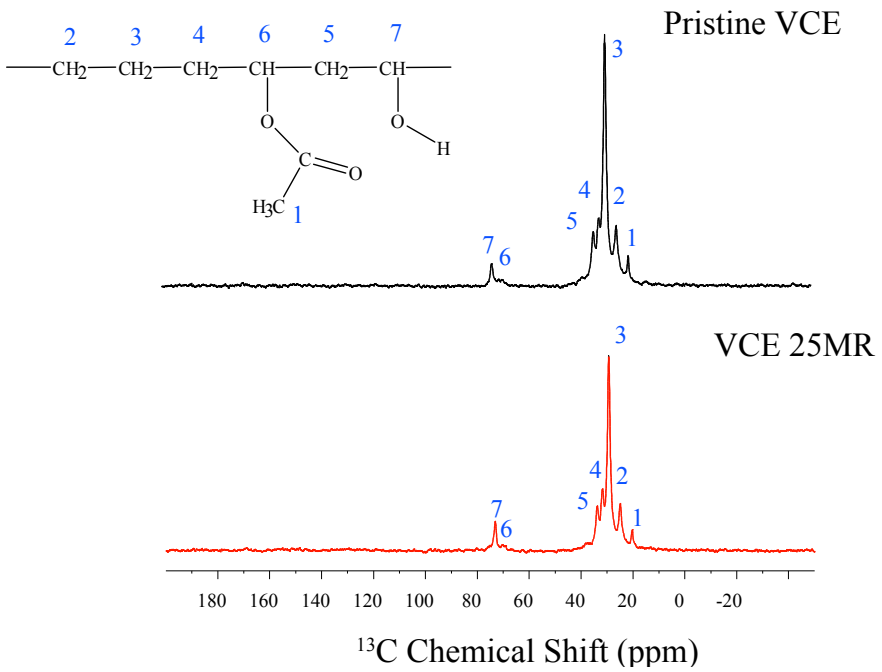

Figure 7: $^{13}C\{^{1}H\}$ CPMAS NMR data on pristine and 25MRad VCE shows small changes in the aliphatic carbon, which are bound to oxygen.

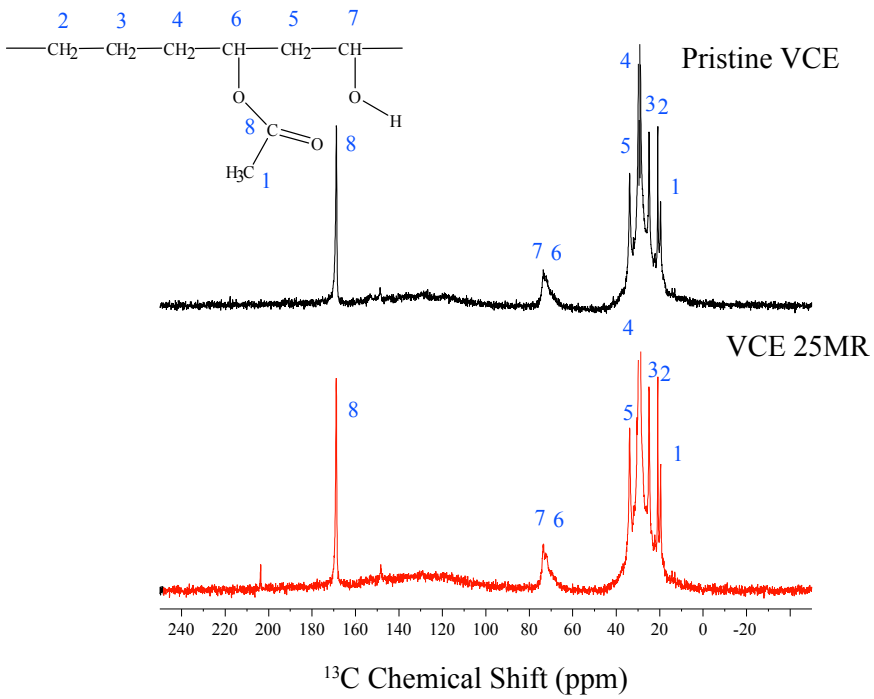

Figure 8: ^{13}C MAS NMR data on pristine and 25MRad VCE shows small changes in the aliphatic carbon, which are bound to oxygen. However, these spectra show no changes to the carboxyl carbons.

To verify the changes in the aliphatic carbon in the form of CH, a 1H MAS NMR experiment was performed on the pristine and 25MR irradiated VCE. These spectra are shown in Figure 9. The 1H MAS spectra of both samples show a peak at 1.98ppm, which represents aliphatic protons in the form of CH_3. In addition, the spectra show a large peak at 1.33ppm, which represent aliphatic protons in the form of CH_2. The 1H MAS NMR spectra for both the pristine and 25MR irradiated VCE show no significant changes in chemical shift or peak shape, indicating that the aliphatic protons are very stable. However, the most substantial change between the pristine and 25MR irradiated sample occurs in the peaks at 4.6ppm and 4.9ppm, which represent the aliphatic protons CH, bound to oxygen, which confirms the changes observed in the 13C MAS NMR data.

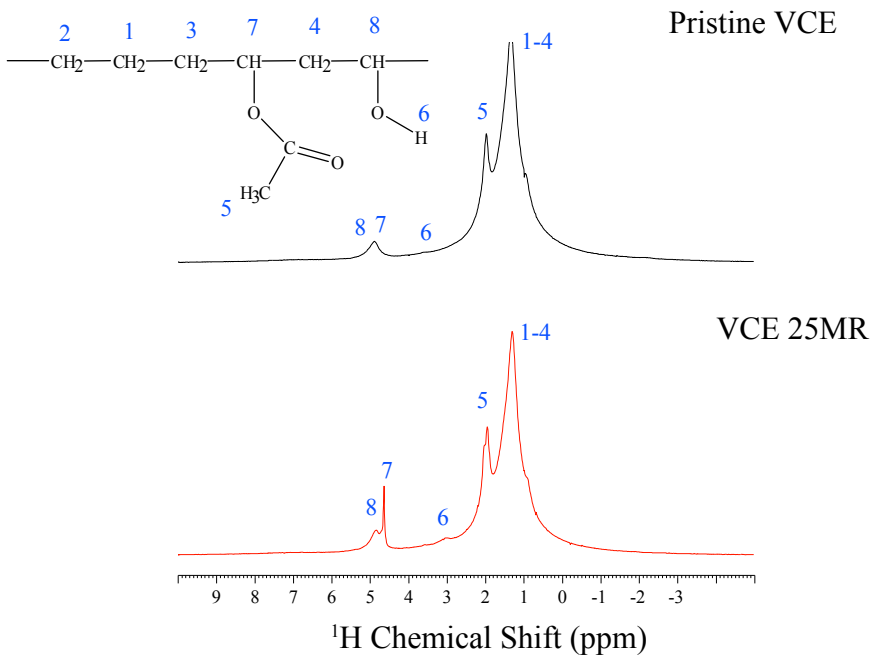

Figure 9: ^{1}H MAS NMR data on pristine and 25MRad VCE show changes in the aliphatic carbon, which are bound to oxygen.

4. Conclusion

We performed initial aging studies of unfilled VCE samples, comparing structural and chemical properties of pristine and irradiated samples under various temperature conditions. The results obtained to date showed that significant temperature degradation only occurs above 300 ºC, with the thermal scission of the acetate group observed at 315 ºC, followed by the thermal degradation of the hydrocarbon backbone at 420 ºC. Structural effects of gamma irradiation in air include reduced crystallinity, reduced uniformity, and increased cross-linking, as determined by DSC. Outgassing measured by SPME-GC-MS showed that acetic acid, phenol, and cyclic siloxanes were given off by the VCE material, and that the abundance of these chemicals was affected by gamma irradiation. Both the ^{13}C and ^{1}H NMR indicate that the backbone structure of VCE is rather stable; however, there exists slight changes in the aliphatic carbons bound to oxygen. This mostly impacts the shape and size of the NMR peaks and not the chemical shifts, which could be caused by dynamical changes in the polymer structure. In order to further understand these effects, we have begun to set up a series of advanced NMR experiments, including Center band-Only Detection of Exchange (CODEX) NMR and Wide-line Separation (WISE) NMR. CODEX NMR is a powerful technique for targeting dynamics in polymeric materials that will enable detailed and qualitative analysis of slow motions [12, 13]. In addition, WISE NMR experiments [14] will enable the correlation of structure and segmental mobility in these complex systems.

5. Future work

The limited amount of material available for this study did not allow mechanical testing. Future studies conducted using new VCE material from KCP will involve repeating the experiments presented in this report and adding thorough mechanical testing, which will provide insight into structural changes, as well as more complex NMR experiments such as Center band-Only Detection of Exchange (CODEX) and Wide-line Separation (WISE) NMR, which provide insight into the dynamical changes in the VCE material as it is exposed to radiation and thermal changes. Filled material will also be studied in the future.

5. References

1. W.E. Cady, *Transition temperatures and crystallinity in EVA, VCE, and Rattan C*, LLNL report UCID-15424 (1969).

2. P.M. Wilson, D.A. Spieker, *Enhanced Surveillance of Filled Elastomers*, KCP report KCP-613-6004 (1997).

3. E.A. Eastwood, D.E. Bowen, *VCE replacement development: characterization of EVA materials*, KCP report KCP-613-6929 (2004).

4. E.A. Eastwood, *VCE replacement development: curing studies*, KCP report KCP-613-8161 (2006).

5. A. Lopez-Rubio, J.M. Lagaron, T. Yamamoto, R. Gavara, *Radiation-induced oxygen scavenging activity in EVOH copolymers*, Journal of Applied Polymer Science 105, 2676-2682 (2007).

6. Y. B. Byun, S.I. Hong, K.B. Kim, D.H. Jeon, J.M. KIM, W.S. Whiteside, H.J. Park, *Physical and chemical properties of gamma-irradiated EVOH film*, Radiation Physocs and Chemistry 76, 974-981 (2007).

7. P. Budrugeac, T. Zaharescu, M. Marcuta, Gh. Marin, *Accelerated electron effects on EVA based compound*, Journal of applied polymer science 96, 613-617 (2005).

8. W.-A. Zhang, Y.-E. Fang, *Enhancement of radiation-resistant effect in ethylene vinyl acetate copolymers by the formation of ethylene vinyl acetate copolymers/clay nanocomposites,* Journal of applied polymer science 98, 2532-2538 (2005).

9. E. Perez, M. Lujan, J. Martinez de Salazar, *Preparation and properties of terpolymers of ethylene, vinyl acetate and vinyl alcohol*, Macromolecular chemistry and physics 201, 1323-1328 (2000).

10. M. VarmaNair, B. Wunderlich, *Heat-capacity and other thermodynamic properties of linear macromolecules. 10. Update of the ATHAS 1980 data-bank*, Journal of physical chemistry 20, 349-404 (1991).

11. D. Marks and S. Vega, *A Theory for Cross Polarization NMR of Nonspinning and Spinning Samples*, Journal of Magnetic Resonance, Series A, 118, 157-172 (1996).

12. E.R. deAzevedo, W.G. Hu, T.J. Bonagamba, and K. Schmidit-Rohr, *Centerband-Only Detection of Exchange: efficient analysis of Dynamics in Solids by NMR*, J. Am. Chem. Soc., 121, 8411-8412 (1999).

13. E.R. deAzevedo, W.G. Hu, T.J. Bonagamba, and K. Schmidit-Rohr, J. *Principles of centerband-only detection of exchange in solid-state nuclear magnetic resonance, and extension to four-time centerband-only detection of exchange,* Journal of Chemical Physics, 112, 8988-9001(2000).

14. K. Schmidit-Rohr, J. Clauss, H.W. Spiess, *Correlation of Structure, Mobility, and Morphological Informatin in Heterogeneous Polymer Materials by Two-Dimensional Wideline-Separation NMR Spectroscopy,* Macromolecules, 25, 3273-3277 (1991).